

MLL-TET1 fusion protein promotes immortalization of myeloid progenitor cells and leukemia development

Mixed lineage leukemia (*MLL*) is involved in maintaining epigenetic transcriptional regulation. An *MLL*-rearranged translocation triggers a broad range of aggressive hematologic malignancies, including acute lymphoblastic leukemia and acute myelogenous leukemia. Such a translocation also confers a poor prognosis compared with that of non-rearranged leukemia.¹⁻³ Reciprocal translocations of the *MLL* gene result in the replacement of the *MLL* 3' coding sequences, with more than 70 translocation partners.^{4,5} Some of these *MLL*-rearranged genes, including *MLL-AF9*, *MLL-AF4*, and *MLL-ENL*, have been extensively studied.⁶ Although *MLL-TET1* (*MT1*) was identified before the other translo-

cations, there have been few investigations of this gene in the context of myeloid malignancy, partly because of the rarity of the *MT1* rearrangement. Recently, *TET1* was observed to play an important role in the epigenetic mechanisms that regulate gene expression, development, and cancer. In addition, *TET1* is a direct target of *MLL-AF9* and *MLL-ENL*, and it plays an oncogenic role with the *MLL*-fusion protein.⁷ Herein, we evaluated the oncogenic potential of the *MT1* fusion protein using *in vivo* and *in vitro* analyses.

An *in vitro* colony-forming/replating assay was performed to determine whether the *MT1* fusion protein, like other *MLL*-rearranged proteins, stimulates immortalization of myeloid progenitor cells. Because most occurrences of *MT1* fusion have been identified in cases of acute myeloid leukemia, we used myeloid progenitor cells to determine the function of *MT1* fusion in only

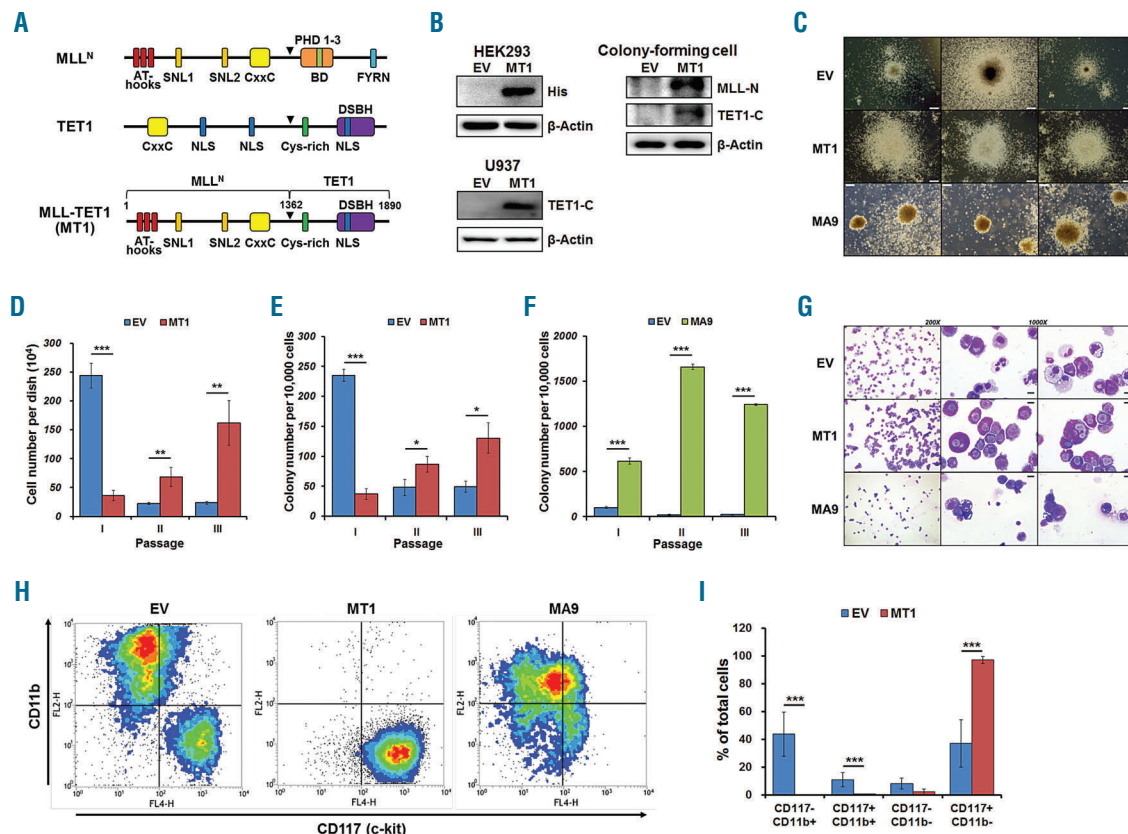


Figure 1. The *MLL-TET1* fusion protein stimulates immortalization of myeloid progenitor cells. (A) Schematic representation of the human *MLL* N-terminal, *TET1* C-terminal, and *MLL-TET1* fusion proteins. The vertical arrows indicate the translocational breakpoint. SNL: subnuclear localization motif; CxxC: zinc-binding CxxC domain; PHD: plant homeodomain; BD: bromodomain; FYRN: FY-rich domain N-terminal; NLS: nuclear localization signal; and DSBH, double-stranded β -helix-2OG-Fe(II)-dependent dioxygenase are designated. (B) *MT1* protein expression compared with that of the empty vector (EV) was determined in HEK293, U937, and colony-forming cells by western blot analysis. Anti-*MLL-N* recognized the N-terminal fragment of *MLL* generated by proteolytic cleavage. Anti-*TET1-C* recognized the peptide mapping near the C-terminus of *TET1*. β -actin was used as a loading control. (C) The myeloid progenitor cells of the mice were transduced with an empty vector (EV) or with the *MLL-TET1* (*MT1*) or *MLL-AF9* (*MA9*) fusion expression vector and differentiated respectively into the myeloid lineage using cytokine treatments (stem cell factor, interleukin-3, interleukin-6, granulocyte colony-stimulating factor). Colony morphology was analyzed with an IX51 microscope. The scale bar represents 100 μ m. The human *MT1* fusion induced immortalization of myeloid progenitor cell in the mice. The numbers of the cells (D) and colonies (E) that were transformed with EV or *MT1* are displayed (* $P < 0.05$, ** $P < 0.01$ and *** $P < 0.001$; data are presented as the mean \pm SD). (F) The number of colonies for the cells transformed with the empty vector (EV) or *MLL-AF9* (*MA9*) are displayed (*** $P < 0.001$; data are presented as the mean \pm SD). (G) Representative images of the cytopsin preparations in the secondary passage of the colony-forming assay. Most of the *MT1*-transduced cells were immature cells in contrast to the presence of mature macrophages and segmented neutrophils in the EV-transduced cells. The scale bar represents 10 μ m. (H, I) Flow cytometric analyzes of the EV-, *MT1*-, or *MA9*-transduced colony-forming cells. The colony-forming cells in the secondary passage were stained with APC-labeled anti-CD117 (c-kit) antibodies and PE-labeled anti-CD11b (Mac-1) antibodies. The *MT1*-transduced cells had a much higher proportion of CD117⁺CD11b⁻ cells compared with that of the EV-transduced cells (*** $P < 0.001$; data are presented as the mean \pm SD).

myeloid lineages.⁸⁻¹⁰ We induced the myeloid progenitor cells by growing murine bone marrow mononuclear cells with Iscove modified Dulbecco medium containing 15% fetal bovine serum, interleukin-3, interleukin-6 and stem cell factor for 48 h. During this period, mononuclear cells were activated into myeloid progenitor cells and the number of myeloid progenitor cells was increased. The breakpoint region of the MT1 fusion between exon 9 of MLL and exon 9 of TET1 has been previously identified (Figure 1A).¹¹ The expression of the MT1 fusion protein was confirmed using antibodies against the polyhistidine tag, TET1 C-terminus, and MLL N-terminus in HEK293, U937, and colony-forming cells, respectively (Figure 1B). The empty vector (EV)- and the *MT1*-transduced progenitor cells (10,000 cells each) were plated onto a methylcellulose medium containing myeloid differentiation factors. The colony formation assays revealed that the *MT1*-transduced colonies were widely spread with an undifferentiated shape and were maintained at replating compared to tightly packed *MA9*-transduced colonies (Figure 1C). The number of the *MT1*-transduced colonies and cells increased significantly

($P < 0.05$) after a second round of replating compared with that of the EV-transduced colonies, but the number was substantially lower than that of the *MA9*-transduced colonies (Figure 1D-F). In addition, cytospin analyses of the colony-forming cells demonstrated that all of the *MT1*- and *MA9*-transduced cells displayed a maturation arrest in contrast to the higher proportion of mature macrophages and segmented neutrophils in the EV-transduced cells (Figure 1G,H). Flow cytometry revealed that the *MT1*-transduced cells exhibited a much higher proportion of CD117⁺ (hematopoietic progenitor cell marker) and CD11b⁺ (myeloid mature cell marker) cells than did the EV-transduced cells (95% versus 37%, respectively, $P < 0.001$; Figure 1H,I).

To determine whether *MT1* suppressed differentiation *in vivo* and *in vitro*, mice bone marrow transplantation (BMT) assays were performed with GFP-tagged and *MT1*-transduced myeloid progenitor cells. Eight-week old C57BL/6 recipient mice were lethally irradiated (¹³⁷Cs) at a dose of 8 Gy. The unsorted retrovirus-transduced myeloid progenitor cells (1.5×10^6 per mouse, the efficiency of transduction was 15–20%) were transplanted

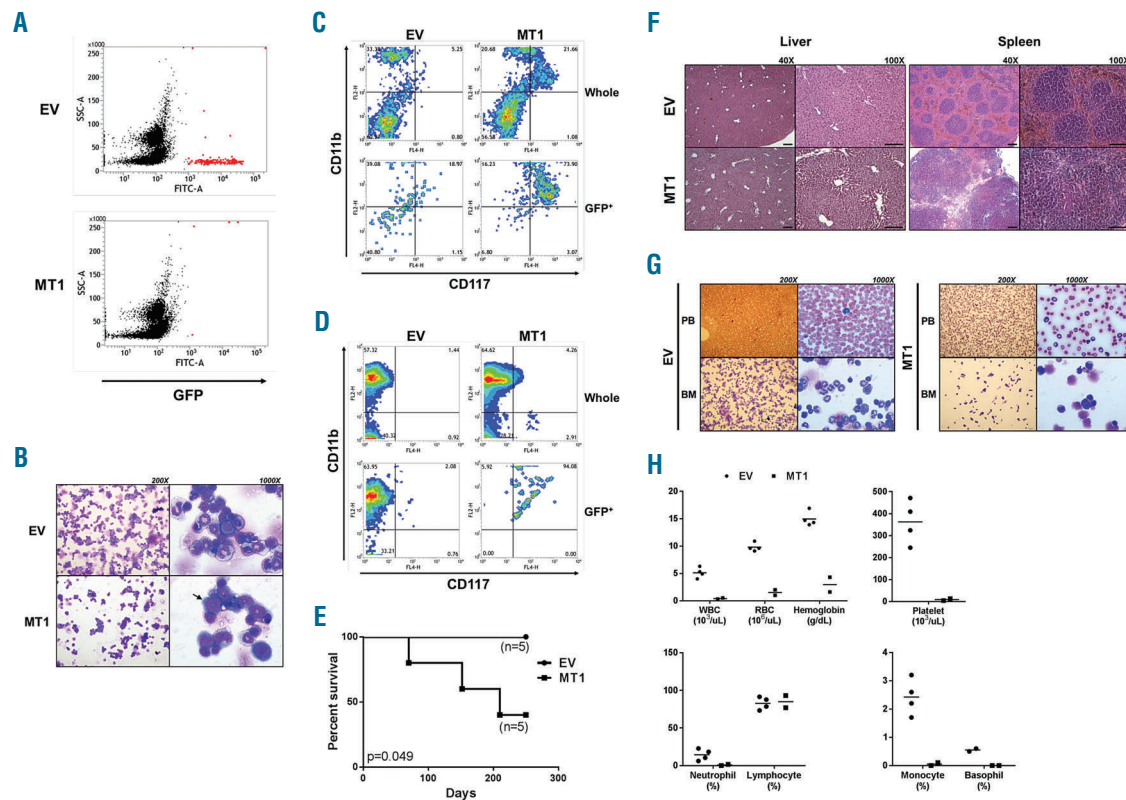


Figure 2. The MLL-TET1 suppresses the differentiation of myeloid progenitor cells *in vivo*. (A) The differentiation of myeloid progenitor cells was assessed using flow cytometry in the peripheral blood of the EV ($n=3$) and *MT1* ($n=5$) transplanted mice. The red spot indicates GFP-positive cells in the peripheral blood of the bone marrow transplanted mice. (B) Representative images of the cytospin preparations from the bone marrow at 20 days after the BMT. The morphologies of the bone marrow cells in the mice transplanted with the EV- or *MT1*-transduced bone marrow cells were identified by cytospin. In the *MT1*-transduced bone marrow, clusters of immature cells were frequently noted (black arrow). (C) Flow cytometric analysis of the bone marrow at 20 d after the BMT. (D) Flow cytometric analysis of the bone marrow at 50 d after the BMT. The bone marrow cells in the transplanted mice were stained with APC-labeled anti-CD117 (c-kit) antibodies and PE-labeled anti-CD11b (Mac-1) antibodies. The EV- and *MT1*-transduced cells were identified by GFP expression. (E) The Kaplan–Meier survival curve for the EV- and *MT1*-transduced bone marrow recipients. (F) Representative images of the liver and spleen in the EV and *MT1*-transduced bone marrow recipients at 152 days after the BMT. The scale bar represents 200 μm . (G) The peripheral blood (PB) and the bone marrow were extracted from healthy EV-transduced bone marrow recipients and from *MT1*-transduced bone marrow recipients that displayed signs of imminent death at 152 days after the BMT. (H) The numbers of white blood cells, red blood cells, hemoglobin, and platelets and the percentages of neutrophils, lymphocytes, monocytes, and basophils, were determined from the peripheral blood of EV-transduced bone marrow recipients ($n=4$) and *MT1*-transduced bone marrow recipients ($n=2$) by using the Sysmex XE-5000 hematology analyzer (Sysmex Corporation Kobe, Japan). The EV- and *MT1*-transduced bone marrow recipients were transplanted from two independent cohorts with independent virus preparations.

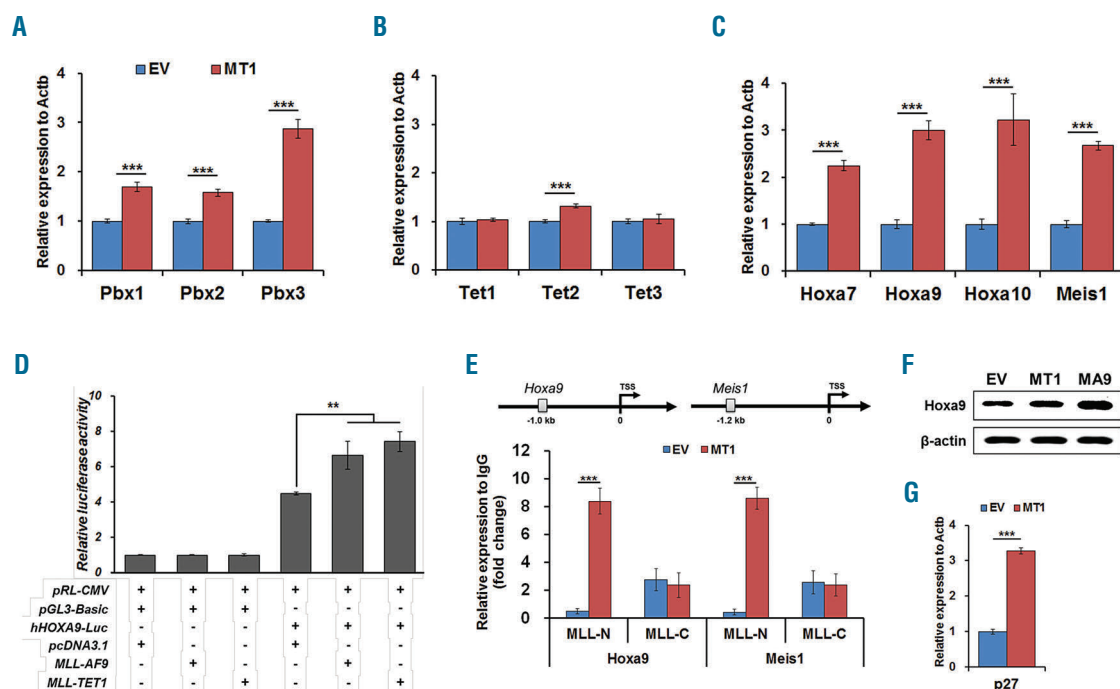


Figure 3. The MLL-TET1 fusion increases the expression of leukemogenic genes. The expression levels of the (A) *Pbx* family members (B) *Tet2* of the *Tet* family and the (C) *Hoxa* family members and *Meis1* were increased (mean \pm SD, *** P <0.001) compared with those of the control cells. (D) Luciferase reporter assays of the human *HOXA9* promoter regions. The pcDNA3.1 (empty vector), *MT1*, *MA9*, or *pRL-CMV* (pRL *Renilla reniformis* luciferase control reporter vector, internal control) was transiently transfected into RAW264.7 cells. The fold change relative to the pGL3-basic firefly luciferase reporter vector is displayed (mean \pm SD, ** P <0.01). (E) The chromatin immunoprecipitation real-time polymerase chain reaction assay of MLL-N and MLL-C binding to the *Hoxa9* and *Meis1* promoter regions. The EV- or *MT1*-transduced colony-forming cells were immunoprecipitated using anti-MLL-N, anti-MLL-C, and normal IgG control antibodies. MLL-N and MLL N-terminal represented both the wild-type MLL and the MLL-fusion proteins. The MLL-C and MLL C-terminal represented the wild-type MLL only. (F) *Hoxa9* protein expression was increased in the *MT1*- and *MA9*-transduced colony-forming cells. (G) The expression level of p27kip1 was increased in the secondary passage of *MT1*-transduced colony-forming cells (mean \pm SD, *** P <0.001).

into the irradiated C57BL/6 congenic mice by direct intrafemoral injection. Shortly after the BMT (20 days), a significant proportion of GFP-positive peripheral blood cells was observed, but only in the EV cell-BMT mice (Figure 2A). However, the bone marrow of EV cell-BMT mice revealed a normal maturation sequence, while that of *MT1* cell-BMT mice revealed myeloid maturation arrest with clusters of immature cells (Figure 2B). In addition, the proportion of CD11b⁺CD117⁺ in the GFP-positive cells in the bone marrow of the *MT1* cell-BMT mice was greater than that in the bone marrow of the EV cell-BMT mice (73.90% versus 18.97%; Figure 2C). To assess the ongoing activities of the *MT1* cells *in vivo*, bone marrow was extracted and analyzed at 50 days after the BMT. Among the total cell populations, the bone marrow of the *MT1* cell-BMT mice displayed slightly higher percentages of CD11b⁺CD117⁺ than did that of the EV-BMT mice (4.26% versus 1.44%; Figure 2D). Although the proportion of GFP-positive cells in the bone marrow of *MT1* -BMT mice at 50 days was lower than at 20 days after the BMT, the GFP-positive cells in the *MT1*-BMT BM contained a much larger proportion of CD11b⁺CD117⁺ cells compared with those in the EV-BMT bone marrow (94.08% versus 2.08%; Figure 2D). The Kaplan-Meier survival curves of the EV- and the *MT1*-BMT recipients 300 days after the BMT indicated that the *MT1* overexpression reduced the overall survival ($P=0.049$, log-rank test, Figure 2E). The central veins and the pericentral sinusoids in the liver of the *MT1*-BMT mice were severely dilated, and their splenic architecture was dis-

rupted and infiltrated by immature cells (Figure 2F). In addition, the peripheral blood of the *MT1*-BMT mice showed signs of cell death and demonstrated pancytopenia and agranulocytosis, and the bone marrow was replaced by immature blasts (Figure 2G). However, the percentages of lymphocytes were sustained. The hemoglobin and numbers of myeloid lineage cells, such as white blood cells, red blood cells, platelets, neutrophils, monocytes, and basophils, were all decreased in the peripheral blood of the *MT1*-BMT recipients at 70 days and 152 days after the BMT. These were signs of imminent death (Figure 2H).

We next analyzed the levels of leukemogenic gene expression in the *MT1*-transduced cells by using quantitative real-time polymerase chain reaction. All members of the *Pbx* family were substantially up-regulated following *MT1* overexpression, and *Tet2* of the *Tet* family was slightly increased (Figures 3A,B). In addition, *MT1* significantly augmented the expression levels of the *Hoxa7*, *Hoxa9*, *Hoxa10*, and *Meis1* genes (Figure 3C). *MT1* and *MA9* stimulated human *Hoxa9* promoter activities in RAW264.7 cells (Figure 3D). The abundance of the *Hoxa9* and *Meis1* promoter regions in MLL-N and MLL-C precipitated DNA from the *MT1*-transduced cells. This increased significantly relative to that of control (Figures 3E). It is important to note that the *MT1* fusion protein only contained the MLL-N terminus of MLL. *Hoxa9* and *Meis1* are target genes of the MLL fusion protein in MLL-rearranged leukemia and they are important factors in the initiation of leukemia. The protein expres-

sion of Hoxa9 in the *MT1*-transduced cells was increased compared to that in the EV-transduced cells, but levels were lower than those in the *MA9*-transduced cells (Figures 3F). In addition, the expression level of p27^{kip1}, a negative regulator of the cell cycle, was augmented in *MT1*-transduced cells compared to the level in EV-transduced cells (Figure 3G).

In the present study, we report that the *MT1*-fusion stimulated immortalization and inhibited the differentiation of the myeloid progenitor and transplanted bone marrow cells. Interestingly, the surface markers of *MT1*-transduced myeloid progenitor cells *in vitro* were CD117⁺CD11b⁻, and the surface markers of most of the *MT1* leukemic cells recovered after the BMT changed to CD117⁺CD11b⁺. Previous studies showed that when BMT was performed using CD117⁺CD11b^{hi} or CD117⁺CD11b^{lo} *MA9* leukemic cells, AML developed at similar times and showed the same phenotype and similar percentages of surface markers. This indicates the possibility of a phenotypic inter-convertibility between CD117⁺CD11b^{hi} and CD117⁺CD11b^{lo} *MA9* leukemic cells.¹² The above phenomenon appears to have also occurred in *MT1* cells.

The colony-forming assay showed that the *MT1*-transduced colonies and cells increased significantly compared to the control. However, the proliferation rate of immortalized *MT1*-transduced colonies was slower than that of *MA9*-transduced colonies. In addition, BMT analysis showed that the leukemia with *MT1* develops slower than that with *MA9*. It is known that the proliferation rate of cells increases with the progression of differentiation from hematopoietic stem cells to terminal cells and in the case of common myeloid progenitors, megakaryocyte-erythroid progenitors, and granulocyte-macrophage progenitors, the proliferation rate is two to three times higher than that of multipotent progenitors. It is also known that CD117⁺CD11b^{lo} cells account for 1~3% of *MA9* leukemic cells, which are relatively quiescent compared to CD117⁺CD11b^{hi} cells and the majority of them remain in the G0/G1 stage. These characteristics are closely related to the expression of p27, and the expression of p27 is relatively higher in CD117⁺CD11b^{lo} *MA9* leukemic cells than in CD117⁺CD11b^{hi} cells. In addition, p27 inhibits leukemic cell proliferation with *MYC* and is known to play a central role in the maintenance of quiescence and drug resistance in CD117⁺CD11b^{lo} *MA9* cells. CD117⁺CD11b⁻ *MT1* transduced cells are, therefore, more likely to grow slowly than CD11b⁺ *MA9* transduced cells and may also take longer to develop leukemia.

We investigated the leukemogenic potential of *MT1* using *in vivo* and *in vitro* analyses. In order to understand the mechanism of leukemia induction by *MT1*, functional studies to evaluate factors such as differentiation and the cell cycle will be required, and comparison with other cases of *MLL* rearranged acute myelogenous leukemia will provide new insights.

Hyung-Soo Kim,^{1,2} Seung Hwan Oh,³ Ju-Heon Kim,⁴ Jae-Young Kim,⁴ Do-Hyung Kim,⁵ Soo-Jin Lee,⁶

Sang-Un Choi,⁷ Kwon Moo Park,⁸ Zae Young Ryou,¹ Tae Sung Park⁹ and Sanggyu Lee¹

¹School of Life Science, BK21 plus KNU Creative BioResearch Group, Kyungpook National University; ²Institute of Life Science and Biotechnology, Kyungpook National University; ³Department of Laboratory Medicine, College of Medicine, Inje University; ⁴Department of Biochemistry, School of Dentistry, IHBR, Kyungpook National University; ⁵Department of Physics, Kyungpook National University; ⁶Department of Occupational and Environmental Medicine, Hanyang University College of Medicine; ⁷Korea Research Institute of Chemical Technology; ⁸Department of Anatomy, Kyungpook National University School of Medicine and ⁹Department of Laboratory Medicine, Kyung Hee University School of Medicine, Seoul, Republic of Korea

Funding: this study was supported by grant SI1706 (Development of Radio-Modulators for Radio Accidents) by the Korea Research Institute of Chemical Technology (KRICT) and the National Research Foundation of Korea (grant NRF-2016R1C1B1010734) funded by the Ministry of Education, Science and Technology, Republic of Korea.

Correspondence: slee@knu.ac.kr
doi:10.3324/haematol.2017.169789

Information on authorship, contributions, and financial & other disclosures was provided by the authors and is available with the online version of this article at www.haematologica.org.

References

1. Ayton PM, Cleary ML. Molecular mechanisms of leukemogenesis mediated by MLL fusion proteins. *Oncogene*. 2001;20(40):5695-5707.
2. Hess JL. MLL: a histone methyltransferase disrupted in leukemia. *Trends Mol Med*. 2004;10(10):500-507.
3. Muntean AG, Hess JL. The pathogenesis of mixed-lineage leukemia. *Annu Rev Pathol*. 2012;7:283-301.
4. Caslini C, Sema A, Rossi V, Introna M, Biondi A. Modulation of cell cycle by graded expression of MLL-AF4 fusion oncoprotein. *Leukemia*. 2004;18(6):1064-1071.
5. Gu Y, Alder H, Nakamura T, et al. Sequence analysis of the breakpoint cluster region in the ALL-1 gene involved in acute leukemia. *Cancer Res*. 1994;54(9):2327-2330.
6. Meyer C, Hofmann J, Burmeister T, et al. The MLL recombinome of acute leukemias in 2013. *Leukemia*. 2013;27(11):2165-2176.
7. Huang H, Jiang X, Li Z, et al. TET1 plays an essential oncogenic role in MLL-rearranged leukemia. *Proc Natl Acad Sci USA*. 2013; 110(29):11994-11999.
8. Burmeister T, Meyer C, Schwartz S, et al. The MLL recombinome of adult CD10-negative B-cell precursor acute lymphoblastic leukemia: results from the GMALL study group. *Blood*. 2009;113(17):4011-4015.
9. Ittel A, Jeandidier E, Helias C, et al. First description of the t(10;11)(q22;q23)/MLL-TET1 translocation in a T-cell lymphoblastic lymphoma, with subsequent lineage switch to acute myelomonocytic myeloid leukemia. *Haematologica*. 2013;98(12):e166-168.
10. Lee SG, Cho SY, Kim MJ, et al. Genomic breakpoints and clinical features of MLL-TET1 rearrangement in acute leukemias. *Haematologica*. 2013;98(4):e55-57.
11. Lorsbach RB, Moore J, Mathew S, Raimondi SC, Mukatira ST, Downing JR. TET1, a member of a novel protein family, is fused to MLL in acute myeloid leukemia containing the t(10;11)(q22;q23). *Leukemia*. 2003;17(3):637-641.
12. Zhang J, Seet CS, Sun C, et al. p27kip1 maintains a subset of leukemia stem cells in the quiescent state in murine MLL-leukemia. *Mol Oncol*. 2013;7(6):1069-1082.